Neurobiology of Disease

In Vivo Diffusion Tensor Imaging and Histopathology of the Fimbria-Fornix in Temporal Lobe Epilepsy

Luis Concha,[1] Daniel J. Livy,[2] Christian Beaulieu,[1]* B. Matt Wheatley,[3] and Donald W. Gross[4]*

[1]Department of Biomedical Engineering, [2]Faculty of Medicine and Dentistry, Division of Anatomy, [3]Department of Surgery, Division of Neurosurgery, and [4]Department of Medicine, Division of Neurology, University of Alberta, Edmonton, Alberta, Canada T6G 2B7

While diffusion tensor imaging (DTI) has been extensively used to infer micro-structural characteristics of cerebral white matter in human conditions, correlations between human *in vivo* DTI and histology have not been performed. Temporal lobe epilepsy (TLE) patients with mesial temporal sclerosis (MTS) have abnormal DTI parameters of the fimbria-fornix (relative to TLE patients without MTS) which are presumed to represent differences in axonal/myelin integrity. Medically intractable TLE patients who undergo temporal lobe resection including the fimbria-fornix provide a unique opportunity to study the anatomical correlates of water diffusion abnormalities in freshly excised tissue. Eleven patients with medically intractable TLE were recruited (six with and five without MTS) for presurgical DTI followed by surgical excision of a small specimen of the fimbria-fornix which was processed for electron microscopy. Blinded quantitative analysis of the microphotographs included axonal diameter, density and area, cumulative axon membrane circumference, and myelin thickness and area. As predicted by DTI the fimbria-fornix of TLE patients with MTS had increased extra-axonal fraction, and reduced cumulative axonal membrane circumference and myelin area. Consistent with the animal literature, water diffusion anisotropy over the crus of the fimbria-fornix was strongly correlated with axonal membranes (cumulative membrane circumference) within the surgical specimen (~15% of what was analyzed with DTI). The demonstration of a correlation between histology and human *in vivo* DTI, in combination with the observation that *in vivo* DTI accurately predicted white matter abnormalities in a human disease condition, provides strong validation of the application of DTI as a noninvasive marker of white matter pathology.

Introduction

Diffusion tensor imaging (DTI) is a novel magnetic resonance imaging (MRI) technique that provides a noninvasive window into brain micro-structure via the analysis of the diffusion properties of water (Basser et al., 1994). Based on animal studies, it is generally accepted that the degree of axon packing and myelin sheaths are the main features that cause water diffusion to be anisotropic (Beaulieu, 2002). As a noninvasive marker of white matter pathology, DTI has tremendous potential and has been extensively used to infer the micro-structural characteristics of brain tissue in a myriad of human conditions, including normal development and aging, and neurological and psychiatric disorders (Johansen-Berg and Behrens, 2006; Ciccarelli et al., 2008).

Received March 23, 2009; revised Oct. 14, 2009; accepted Nov. 18, 2009.

Operating support was given by the Canadian Institutes of Health Research (D.W.G., C.B., D.J.L.), the Savoy Foundation, and the University of Alberta Hospital Foundation (D.W.G.). Salary support was provided by the Alberta Heritage Foundation for Medical Research (C.B.) and Promep (L.C.). MRI infrastructure was from the Canada Foundation for Innovation, Alberta Science and Research Authority, Alberta Heritage Foundation for Medical Research, and the University of Alberta Hospital Foundation. Electron microscopy was performed at the Biological Sciences Microscopy Unit, University of Alberta. Fiber-tracking software was kindly provided by Drs. Hangyi Jiang and Susumu Mori (National Institutes of Health Grant P41 RR15241-01). The software for quantitative microscopy was built by Beau Sapach, University of Alberta, Edmonton, Alberta, Canada.

*C. Beaulieu and D. W. Gross made equal contributions to this paper.

Correspondence should be addressed to Dr. Donald W. Gross, Division of Neurology, Department of Medicine, 2E3.19 Walter C Mackenzie Health Sciences Centre, Edmonton, AB, Canada T6G 2B7. E-mail: donald.gross@ualberta.ca.

DOI:10.1523/JNEUROSCI.1619-09.2010

 0270-6474/10/300996-07$15.00/0

Despite its wide spread application, there remains a tremendous lack of correlative data between DTI and histology in humans. Correlations between DTI and myelin content and to a lesser extent axon count have been shown in humans, but were based on DTI acquired on postmortem brains of patients with multiple sclerosis (Schmierer et al., 2007). While brains are rapidly fixed in animal studies, this process is typically delayed in human cadavers. Decomposition of brain tissue is observed within hours after death, which can have considerable effects on the diffusion properties of tissue (D'Arceuil et al., 2007), thus limiting the conclusions that can be drawn from postmortem studies. As it is not feasible to procure fresh tissue in the vast majority of diseases that have been studied, performing correlative studies between *in vivo* DTI and histology in humans has remained elusive.

Temporal lobe epilepsy (TLE) is the most common localization related epilepsy syndrome and is often unresponsive to medical therapy. While mesial temporal sclerosis (MTS) is the most commonly observed pathology in TLE, DTI studies have shown white matter abnormalities in several bundles not necessarily limited to the temporal lobe nor the hemisphere ipsilateral to seizure focus (Arfanakis et al., 2002; Gross et al., 2006; Rodrigo et al., 2007; Focke et al., 2008; McDonald et al., 2008; Nilsson et al., 2008; Yogarajah et al., 2008; Schoene-Bake et al., 2009). We have previously demonstrated that TLE patients with unilateral MTS (TLE+uMTS) have DTI abnormalities of the fimbria-fornix (Concha et al., 2005b) that are not observed in TLE patients who do not have MTS (TLE−MTS) (Concha et al., 2009). As medically intractable TLE+uMTS and TLE−MTS patients routinely

Table 1. Temporal lobe epilepsy patient information

	Subject	MTS present[a]	Gender	Age (years)	Disease duration (years)	Hippocampal T2 (ms)[b]	Surgery side	Surgical outcome (Engel class)[c]
TLE + uMTS	1	Yes	F	41	27	129	Right	Ia
	2	Yes	F	57	39	132	Left	Ic
	3	Yes	F	34	12	147	Left	Ia
	4	Yes	F	36	35	149	Left	Ic
	5	Yes	F	36	16	133	Left	Ia
	6	Yes	M	33	5	128	Left	III
TLE−MTS	7	No	M	36	25	109	Left	III
	8	No	F	45	7	106	Left	Ia
	9	No	M	60	12	106	Left	Ia
	10	No	F	57	14	114	Right	Ia
	11	No	F	40	5	113	Left	Ia

[a]MTS based on the surgical histopathology of the hippocampus.

[b]Preoperative evaluation. Normal Hippocampal T2 = 114 ± 3 ms (Concha et al., 2009).

[c]One year follow-up.

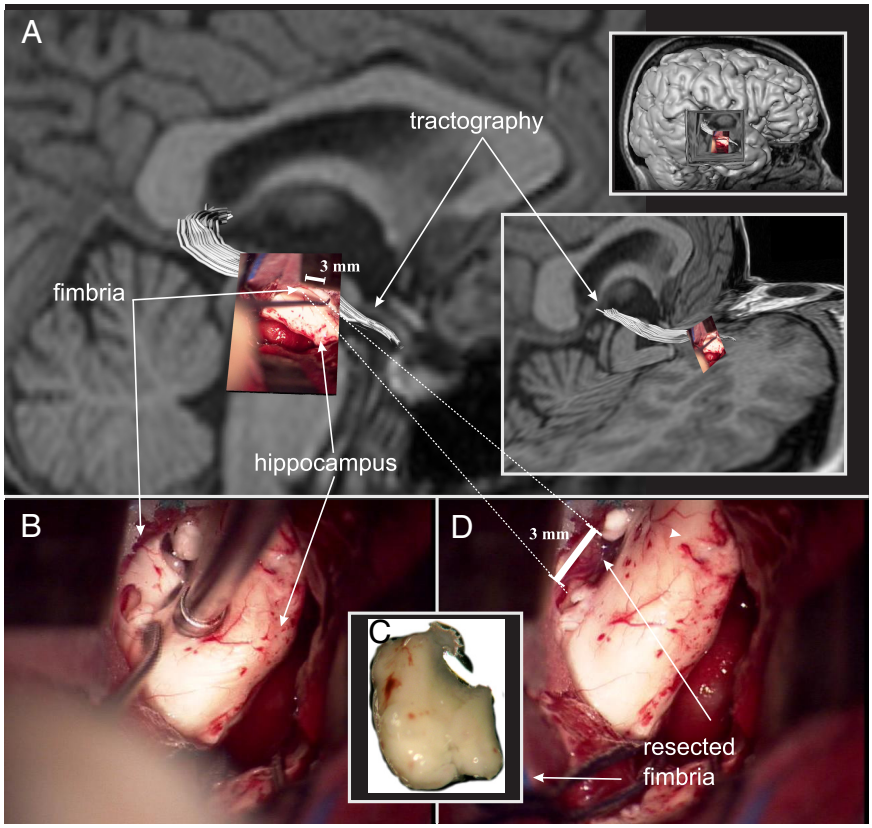

Figure 1. Presurgical tractography and surgical resection of the fimbria-fornix. A photograph of the fimbria-fornix, as seen through the surgical microscope, is overlaid on the preoperative tractography of the same white matter structure (white) (***A***). The fimbria-fornix lies directly above the surgical instrument and the hippocampus as it is being resected (***B***). The specimen has been removed (***C***), leaving a hollow mark above the hippocampus (***D***). The resected specimen is immediately fixed and processed for electron microscopy. Note that the length of the crus of the fimbria-fornix analyzed with DTI (~20 mm) is much larger than the resected specimen used for the electron microscopic quantitative histological analysis (~3 mm, dashed lines).

undergo surgical resection of the temporal lobe (including a portion of the fimbria-fornix) in the management of their condition, this setting provides a unique opportunity to confirm the disruption of myelin/membrane integrity of the fimbria-fornix in patients with TLE+uMTS (as predicted by DTI) and to perform the first correlative study of DTI acquired *in vivo* with subsequent histopathology of a major white matter structure in humans.

The objectives of this study were: (1) to confirm the presence of a unique pathology of the fimbria-fornix in TLE patients with MTS by direct histopathological analysis and (2) to determine the histological features most closely correlated with quantitative water diffusion parameters acquired *in vivo* in humans.

Materials and Methods

Approval of the research protocol was obtained from the University of Alberta Health Research Ethics Board and informed consent was obtained from all participants.

Subjects. Eleven medically intractable TLE patients who were considered good candidates for temporal lobe resection based on presurgical evaluation were recruited for this study (33–60 years old, 8 women). The presurgical evaluation consisted of MRI, interictal and ictal EEG-video telemetry recordings and neuropsychology. Two of 11 subjects (both of which were in the TLE−MTS group) also underwent intracranial EEG-video telemetry before surgery with the intracranial EEG recordings demonstrating unilateral temporal lobe ictal seizure onset. All patients underwent the same imaging protocol preoperatively and were assigned into one of two groups, namely TLE with unilateral MTS (TLE+uMTS) and TLE without MTS (TLE−MTS), based on the histopathology report of the resected hippocampus. All patients presented in this study are a subset from our previous report (Concha et al., 2009). Patient information is provided in Table 1.

Magnetic resonance imaging. Images were acquired on a 1.5T Siemens Sonata MRI scanner. DTI was acquired using a twice-refocused single-shot echoplanar sequence following an inversion pulse (TI = 2200 ms) to suppress the signal arising from cerebrospinal fluid which can negatively impact the quantitative diffusion parameters of the fimbria-fornix (Concha et al., 2005a). Twenty-six contiguous 2 mm thick axial slices were acquired in 9.5 min, providing coverage of the fimbria-fornix, with an in-plane resolution of $2 \times 2\ mm^2$ (data were then interpolated to $1 \times 1 \times 2\ mm^3$). The DTI dataset consisted of eight averages of diffusion-sensitized volumes acquired using six different gradient directions ($b = 1000\ s/mm^2$) and one non-diffusion-weighted volume ($b = 0\ s/mm^2$). Postprocessing of the DTI data was performed with DTIstudio (Johns Hopkins University, Baltimore, MD).

Tractography. The fimbria-fornix on the preoperative DTI was depicted with tractography via the fiber assignment by continuous tracking algorithm (Mori et al., 1999) (Fig. 1). The algorithm initiated streamlines

in all voxels in the brain having a fractional anisotropy (FA) threshold >0.3, and was terminated if the propagating streamlines entered voxels of low anisotropy (FA < 0.3) or deviated by >70°. The fimbria-fornix was virtually dissected by the extraction of those tracts that intersected two manually placed regions of interest (Concha et al., 2005b). Fractional anisotropy was averaged for the voxels lying between the level of the mammillary bodies and the fusion of the crura of the fornices, exactly as we have performed in our previous DTI studies of TLE (Concha et al., 2005a,b, 2009). To further interrogate the basis behind any anisotropy changes, mean diffusivity (MD) and parallel and perpendicular diffusivities of the fimbria-fornix ipsilateral to the seizure focus were also measured for each patient.

Electron microscopy. A segment of the fimbria-fornix, of ~2–5 mm in length, was excised by the neurosurgeon (B.M.W.) with the aid of a surgical microscope (Fig. 1). In all subjects the specimen was obtained from the portion of the fimbria immediately posterior to the head of the hippocampus where the fibers of the alveus converge to form a uniform fiber bundle. The region of the histological specimen was included in the DTI analysis of all subjects making up ~15% of the total region of fimbria-fornix analyzed with DTI. Due to the surgical approach, it was not possible to extract a larger specimen, nor was it possible to acquire a specimen at any other location along the length of the fimbria-fornix. The specimen was immediately prepared for electron microscopy following an established methodology (Livy et al., 1997). Thin tissue sections (90 nm) were cut transverse to the long axis of the fimbria-fornix segment, mounted on 400 mesh copper grids, stained with uranyl acetate and lead citrate, and then viewed and photographed at the approximate middle of the grid pore using an FEI Morgagni transmission electron microscope at a magnification of 3500×. Ten microscopy fields were selected at random blind to subject identification or diagnosis. A random grid pore from the area was selected and photographed, then subsequent fields were photographed by a random movement (for example, 4 grids North, 2 grids East). Due to the nature of electron microscopy, some of the tissue in the target grid pores was of unacceptable quality due to tissue instability caused by the electron beam. These grid pores were skipped and another was selected using the previously mentioned selection method. All the microphotographs were blinded for quantitative evaluation using a nondescriptive numerical code. A stereology counting frame was placed within the microscopic field at 234 nm from its edges, resulting in a counting frame of 364 μm^2. With the aid of an in-house program, the number and inner and outer diameters of axons were manually estimated using an unbiased counting approach and stereology rules (supplemental Fig. 1, available at www.jneurosci.org as supplemental material), yielding 85 ± 25 axons per field. Inner diameter (d_{in}) was defined as the distance between the axonal membranes, whereas outer diameter (d_{out}) was defined as the distance between the outer borders of the myelin sheaths of each axon. Myelin thickness was estimated as $(d_{in} - d_{out})/2$. In the case where noncircular axonal profiles were seen, the diameter was measured based on the shorter axis of the axonal profile. Glial cells, present in some microphotographs, were not counted and their presence did not preclude a microscopy field to be analyzed. The contribution of glial cells to water diffusion anisotropy was not assessed in this study.

Intra-axonal area was given by the sum of the axonal areas (calculated with diameter d_{in} and assuming circular axonal profiles). Myelin area was estimated by the difference in areas of the inner and outer circular profiles of the axons summed over all axons. Extra-axonal area was given as the area not attributed to axons or myelin. All areas are expressed as their ratio to the area of the stereology frame (i.e., intra-axonal fraction + extra-axonal fraction + myelin fraction = 1). Finally, the cumulative axonal membrane circumference was estimated by the sum of all the axonal perimeters calculated with d_{in}. This quantification was performed on each of the 10 microphotographs per patient.

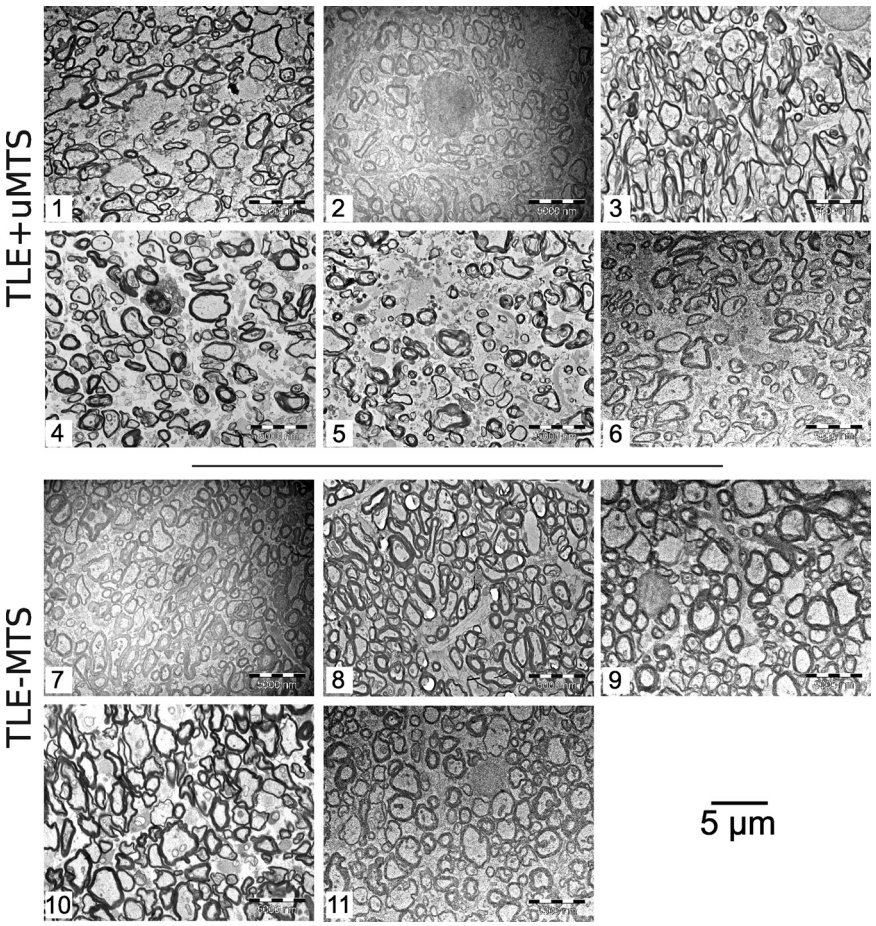

Figure 2. Electron microphotographs of the fimbria-fornix. For each of the six TLE+uMTS and five TLE−MTS patients, one of the 10 available electron microscopy fields is displayed at a magnification of 3500×. Patients with mesial temporal sclerosis show fewer axons and increased extra-axonal space. Patients are identified by numbers (Table 1). Patients 5 and 8 are shown in Figure 3.

The average histological parameters of all microphotographs of each patient were used for statistical analyses. Differences between patients with and without MTS were evaluated using Student's *t* tests, while the correlation between histological characteristics and DTI parameters were evaluated with one-tailed Pearson's correlation coefficient (*r*) including all TLE patients, regardless of the presence of MTS. We performed correction for multiple comparisons for the correlations between histological parameters and FA measurements (our main outcome measure) using the Tukey–Ciminera–Heyse procedure (a variant of the Bonferroni correction) (Tukey et al., 1985; Sankoh et al., 1997). Likewise, correction for multiple comparisons was performed separately for correlations between quantitative histology and MD, parallel and perpendicular diffusivities (i.e., 24 tests), and between-group differences (i.e., 8 tests). Thus, we present both uncorrected and corrected (p_{corr}) *p*-values.

Results

The qualitative blinded assessment of the microphotographs revealed striking morphological differences of the fimbria-fornix of patients with TLE+uMTS compared with TLE−MTS patients (Figs. 2 and 3). It is particularly evident that TLE+uMTS patients exhibit a larger extra-axonal space, with axons that are loosely packed and with greater variability in the size of the axons. The

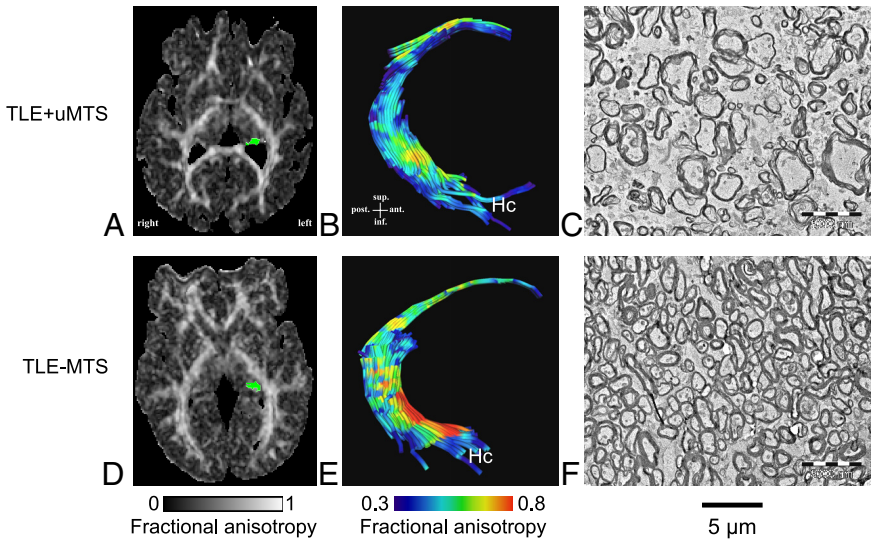

Figure 3. Electron microscopy and tractography of the fimbria-fornix. Histological fields of the fimbria-fornix resected during epilepsy surgery from two representative patients with TLE are shown with their corresponding axial FA maps (***A***, ***D***, with the left fimbria-fornix marked as green) and tractography of the fimbria-fornix (***B***, ***E***). The patient with mesial temporal sclerosis (Patient 5) shows lower diffusion anisotropy of the fimbria-fornix (***B***) than the TLE−MTS (Patient 8) (***E***). This corresponds to lower axonal density and higher extra-axonal fraction (***C***) than in the subject with TLE−MTS (***F***).

Table 2. Group differences in quantitative histology

	TLE+uMTS	TLE−MTS	p	p_{corr}
Axonal density (axons/μm^2)	0.38 (0.04)	0.44 (0.13)	0.054	0.15
Inner axonal diameter (d_{in}, μm)	0.67 (0.07)	0.72 (0.13)	0.4	0.76
Outer axonal diameter (d_{out}, μm)	1.04 (0.05)	1.11 (0.14)	0.27	0.59
Myelin thickness (nm)	186 (13)	194 (25)	0.53	0.88
Cumulative axon membrane circumference (μm)	164 (13)	205 (39)	0.035	0.1
Myelin fraction	0.12 (0.01)	0.15 (0.02)	0.012	0.03
Extra-axonal fraction	0.79 (0.02)	0.72 (0.03)	0.004	0.01
Intra-axonal fraction	0.09 (0.02)	0.13 (0.03)	0.07	0.19

Mean electron microscopy blinded measurements per group are taken from the average features over 10 stereology frames per subject. Numbers in parentheses represent SEM.

myelin sheaths show irregularities in their profiles in TLE+uMTS patients such as separation of myelin layers. Both groups showed an almost complete absence of nonmyelinated axons.

Quantitative blinded analysis of the microphotographs (Table 2) revealed that the extra-axonal fraction best differentiated between the two TLE groups, with TLE+uMTS patients having larger extra-axonal fraction ($p = 0.004$ [$p_{corr} = 0.01$]). The myelin fraction, on the other hand, was significantly different between the two TLE groups, with TLE+uMTS patients showing reduced myelin fraction ($p = 0.012$ [$p_{corr} = 0.03$]), whereas mean myelin thickness did not differ. The cumulative axonal membrane circumference tended to be lower in the TLE+uMTS patients ($p = 0.035$ [$p_{corr} = 0.10$]), as well as the number of axons per field, and thus axonal density ($p = 0.054$ [$p_{corr} = 0.15$]), but there was no difference in axonal diameters.

Histological features derived from electron microscopy of a small specimen of the fimbria-fornix showed significant correlations with FA from the entire ipsilateral crus of the tractography-derived virtual fimbria-fornix in the combined group of 11 TLE patients (Table 3). Fractional anisotropy (Fig. 4) showed a strong positive correlation with the cumulative axonal membrane circumference ($r = 0.71$, $p = 0.007$ [$p_{corr} = 0.02$]). Fractional anisotropy also demonstrated trends toward a positive correlation with axonal density ($r = 0.52$, $p = 0.0495$ [$p_{corr} = 0.13$]), and a negative correlation with myelin thickness ($r = -0.56$, $p = 0.04$ [$p_{corr} = 0.11$]). Mean, parallel and perpendicular diffusivities did not show any significant correlations when corrected for repeated measures with any of the histological features ($p > 0.1$) (Table 3), although a trend was observed for a negative correlation between perpendicular diffusivity and cumulative axonal membrane circumference ($r = -0.61$, $p = 0.02$ [$p_{corr} = 0.11$]) (Fig. 5).

Discussion

As predicted by *in vivo* DTI (Concha et al., 2009), the present study shows direct evidence that TLE+uMTS and TLE−MTS patients have distinctly different histological characteristics of the fimbria-fornix. The most intuitive explanation for histological findings seen in the fimbria-fornix of TLE+uMTS patients is that they reflect downstream degeneration of the output fibers from the mesial temporal region. It must be noted, however, that the fimbria-fornix is a bidirectional pathway, including afferents to the mesial temporal region from a variety of structures including the septum and that other sources of axonal degeneration are also possible. Our previous DTI tractography studies showed bilateral water diffusion abnormalities of the fimbria-fornix in TLE+uMTS patients (Concha et al., 2005b, 2009), in excellent agreement with a recent postmortem study confirming decreased axonal density of the fimbria-fornix bilaterally in four TLE+uMTS patients (Ozdogmus et al., 2009) As ipsilateral but not contralateral fimbria-fornix abnormalities would be expected if the reduced fimbria-fornix integrity was solely secondary to degeneration of mesial temporal efferent fibers, the bilateral findings suggest that degeneration of efferent fibers may not be the only mechanism responsible for the observed changes. Ozdogmus et al. reported that myelinated axons greatly outnumbered unmyelinated axons in the fimbria-fornix of both TLE patients and normal controls (Ozdogmus et al., 2009), while we found a near complete absence of unmyelinated axons in TLE+uMTS and TLE−MTS patients. Given the obvious challenges in acquiring fresh specimens of the fimbria-fornix of control subjects for analysis it is not possible to compare our results to normal controls; however, these results suggest the intriguing possibility that a specific subset of projection fibers may be lost in TLE.

Diffusion tensor imaging has been used to study a large variety of neurological and psychiatric conditions based on the assumption that *in vivo* DTI abnormalities reflect underlying changes in white matter micro-structure. Animal studies have demonstrated that the axonal membranes are primarily responsible for the anisotropic water diffusion observed in peripheral nerves and CNS white matter (for review, see (Beaulieu, 2002). Diffusion MRI studies of giant axons have shown the need of intact membranes for the generation of diffusion anisotropy (Beaulieu and Allen, 1994b; Takahashi et al., 2002). Myelin is not a prerequisite for the presence of diffusion anisotropy (Beaulieu and Allen, 1994a), although myelin sheaths can modulate anisotropy (Gulani et al., 2001; Song et al., 2002, 2003; Harsan et al., 2006; Tyszka et al., 2006; Mac Donald et al., 2007). We demonstrated a

Table 3. Correlations between DTI and quantitative histology

	Axonal density	Inner axonal diameter	Outer axonal diameter	Myelin thickness	Cumulative axon membrane circumference	Myelin fraction	Extra-axonal fraction	Intra-axonal fraction
Fractional anisotropy								
r	0.52	0.15	−0.06	−0.56	0.71	0.27	−0.48	0.48
p	0.0495	0.3	0.4	0.04	0.007	0.2	0.066	0.066
p_{corr}	0.13	0.64	0.76	0.11	0.02	0.47	0.18	0.18
Mean diffusivity								
r	−0.15	−0.27	−0.16	0.29	−0.36	−0.18	0.35	−0.37
p	0.3	0.21	0.3	0.19	0.14	0.3	0.14	0.13
p_{corr}	0.83	0.68	0.83	0.64	0.52	0.83	0.52	0.49
Parallel diffusivity								
r	0.26	−0.2	−0.24	−0.1	0.15	0.03	0.02	−0.04
p	0.2	0.2	0.24	0.4	0.3	0.47	0.48	0.45
p_{corr}	0.66	0.66	0.74	0.92	0.83	0.96	0.96	0.95
Perpendicular diffusivity								
r	−0.39	−0.24	−0.05	0.48	−0.61	−0.27	0.48	−0.48
p	0.12	0.24	0.44	0.067	0.023	0.21	0.065	0.067
p_{corr}	0.47	0.74	0.94	0.29	0.11	0.68	0.28	0.29

Note: Significance after multiple comparisons (p_{corr}) was calculated separately for correlations between quantitative histology and FA (our main outcome measure, 8 correlations), and mean, parallel, and perpendicular diffusivities (24 correlations).

robust positive correlation between FA and cumulative axon membrane circumference, in good agreement with the notion that increased surface area to volume ratio can hinder water diffusion (Latour et al., 1994). Various DTI-histology correlations in animal models have demonstrated relationships of diffusion anisotropy with axonal density and extra-axonal fraction (Takahashi et al., 2002; Schwartz et al., 2005; Wu et al., 2007), although we only found trends with these parameters in our small sample of *in vivo* results in the fimbria-fornix of humans with TLE (Table 3, Fig. 4).

The correlations between the diffusion tensor and histological parameters of human white matter had hitherto only been addressed in the postmortem state. In multiple sclerosis, DTI was demonstrated to correlate with axon counts and myelin (Schmierer et al., 2007, 2008). Recently, it has been shown that postmortem diffusion anisotropy correlates with myelin basic protein in the developing human cerebellum of freshly aborted human fetuses (Saksena et al., 2008). In spasmodic dysphonia, low diffusion anisotropy was found in the internal capsule with postmortem histopathology in a single patient demonstrating axonal loss and decreased myelin content in this region (Simonyan et al., 2008). Although data from animal models and postmortem human brains has provided insight into the histological correlates of DTI parameters, considerable limitations exist in drawing conclusions from these studies regarding the underlying microstructural features associated with human *in vivo* DTI findings. In particular, tissue in postmortem human studies can be assumed to be affected by decomposition before fixation which has been demonstrated to alter both tissue structure as well as DTI parameters (D'Arceuil et al., 2007).

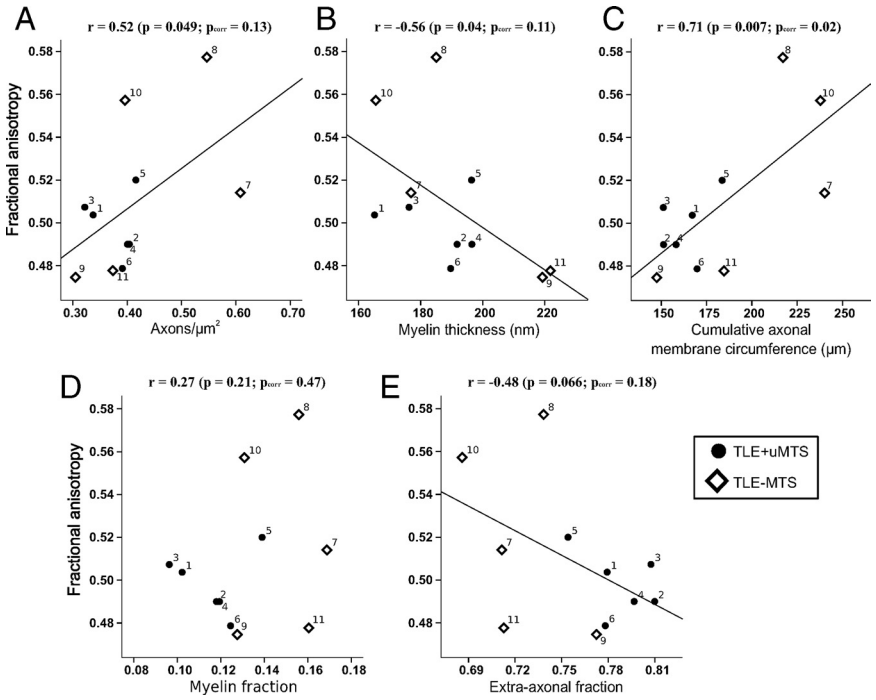

Figure 4. Histological correlates of fractional anisotropy in the fimbria-fornix versus axon density (***A***), myelin thickness (***B***), cumulative axonal membrane circumference (***C***), myelin fraction (***D***), and extra-axonal fraction (***E***). The average fractional anisotropy from the entire ipsilateral crus of the fimbria-fornix and histological parameters from electron microscopy of the smaller specimen of the fimbria-fornix adjacent to the hippocampus are plotted for each subject. FA shows the strongest correlation with cumulative axonal membrane circumference (***C***), namely a positive correlation indicating that anisotropy increases with greater surface area of the axonal membranes. Numbers identify each patient (Table 1).

It is important to recognize that the region of the fimbria-fornix studied with DTI for each subject, ~20 mm in length, was larger than the specimen obtained for histology, ~3 mm resected (illustrated in Fig. 1). Our previous DTI tractography studies of temporal lobe epilepsy used the same methodology presented here for extracting the entire crus of the fimbria-fornix has demonstrated robust differences of TLE+uMTS patients with both controls (Concha et al., 2005b) and TLE−MTS patients (Concha et al., 2009). Averaging over the voxels of the entire crus has two

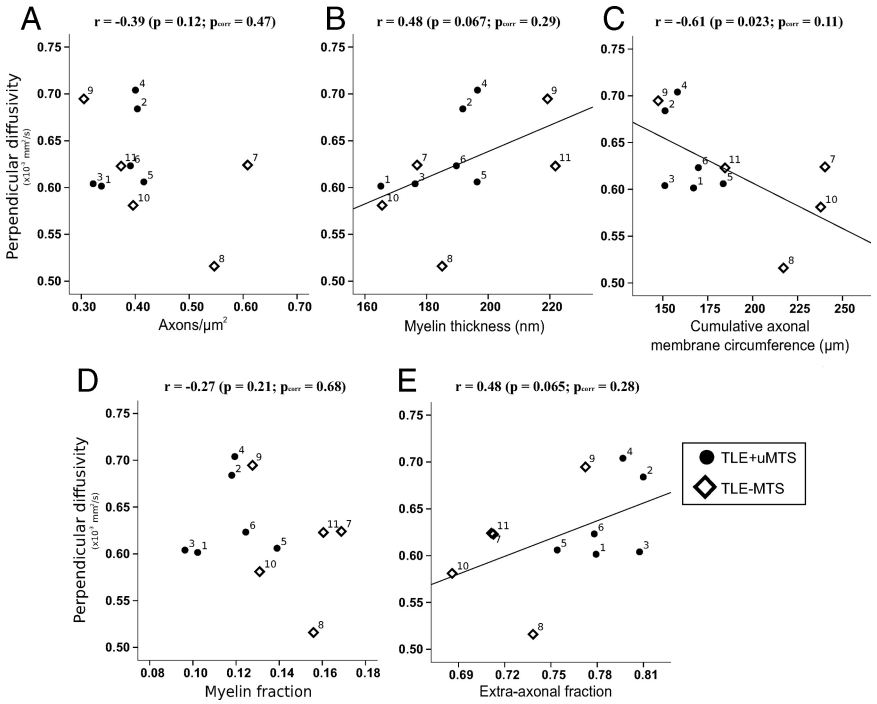

Figure 5. Histological correlates of perpendicular diffusivity in the fimbria-fornix versus axon density (***A***), myelin thickness (***B***), cumulative membrane circumference (***C***), myelin fraction (***D***), and extra-axonal fraction (***E***). Cumulative axonal membrane circumference (***C***) from electron microscopy of the smaller specimen of the fimbria-fornix adjacent to the hippocampus shows a trend toward a negative correlation with perpendicular diffusivity from the entire ipsilateral crus of the fimbria-fornix. The perpendicular diffusion appears to be driving the anisotropy changes reported in Figure 4*C*. Numbers identify each patient (Table 1).

inherent benefits: (1) to help overcome parameter variability as DTI is a low signal-to-noise method, made worse by the use of inversion recovery to suppress signal from CSF and the fact that the fimbria-fornix is a very thin tract, and (2) to provide a summary parameter over the entire presumably contiguous structure as the FA values are not identical along the tract (Fig. 3*B*,*E*), either due to actual biological variability, partial volume averaging given the low resolution of DTI, or noise, as mentioned above. In addition, often areas of very low anisotropy are not measured due to the thresholds used for deterministic streamline tractography. Although DTI analysis of the virtual tract more precisely matched to the histological specimen would have been optimal, several technical issues come into play. First, as mentioned above, the limited number of voxels would have led to more variable DTI parameters per individual. Second, DTI measurements of the fimbria-fornix immediately adjacent to the hippocampus (i.e., the anterior region where the fimbria-fornix was resected) may be variable, as this is where the fibers are coming together (as seen in an electron microphotographs in supplemental Fig. 2, available at www.jneurosci.org as supplemental material). The diffusion tensor model can only be assumed to be an accurate representation of water diffusion if the fibers within a voxel have uniform directionality, but this may not be the case in the resected region where bending fibers could have a major impact on the measurement of diffusion anisotropy. The crus of the fimbria-fornix is more coherent further along the tract, however, this region is not available for histological analysis. For the electron microscopy analysis, we assume that variable fiber orientation would have less of an impact as circular morphology was assumed and axon diameter was measured based on the shortest diameter. As well, only subfields in the electron microscopy microphotographs that were deemed to be perpendicular to the fibers were measured for the histological analysis. We therefore chose to focus on the correlations between the broader DTI analysis and the restricted histological analysis with our assumption being that, since the fibers of the fimbria-fornix are continuous, the pathological processes would likely extend throughout the entire structure and that the broader DTI analysis would provide a more accurate representation of the structural state of the fimbria-fornix as a whole. Further studies with larger sample sizes, albeit not an easy task given the need to acquire presurgical DTI and then obtain an intact white matter tract specimen during neurosurgery, as well as the acquisition of DTI with better resolution and greater signal-to-noise at higher fields are required for confirmation of our results.

This study shows, for the first time in live humans, the relation between tissue morphology and the diffusion parameters obtained noninvasively with DTI in a major white matter tract of human brain. The demonstration of histological differences of the fimbria-fornix between TLE patients with and without MTS, which were predicted based on *in vivo* DTI (Concha et al., 2009), further validates the idea that DTI can be used to investigate white matter tissue characteristics at the microscopic level.

References

Arfanakis K, Hermann BP, Rogers BP, Carew JD, Seidenberg M, Meyerand ME (2002) Diffusion tensor MRI in temporal lobe epilepsy. Magn Reson Imaging 20:511–519.

Basser PJ, Mattiello J, LeBihan D (1994) MR diffusion tensor spectroscopy and imaging. Biophys J 66:259–267.

Beaulieu C (2002) The basis of anisotropic water diffusion in the nervous system-a technical review. NMR Biomed 15:435–455.

Beaulieu C, Allen PS (1994a) Determinants of anisotropic water diffusion in nerves. Magn Reson Med 31:394–400.

Beaulieu C, Allen PS (1994b) Water diffusion in the giant axon of the squid: implications for diffusion-weighted MRI of the nervous system. Magn Reson Med 32:579–583.

Ciccarelli O, Catani M, Johansen-Berg H, Clark C, Thompson A (2008) Diffusion-based tractography in neurological disorders: concepts, applications, and future developments. Lancet Neurol 7:715–727.

Concha L, Gross DW, Beaulieu C (2005a) Diffusion tensor tractography of the limbic system. AJNR Am J Neuroradiol 26:2267–2274.

Concha L, Beaulieu C, Gross DW (2005b) Bilateral limbic diffusion abnormalities in unilateral temporal lobe epilepsy. Ann Neurol 57:188–196.

Concha L, Beaulieu C, Collins DL, Gross DW (2009) White matter diffusion abnormalities in temporal lobe epilepsy with and without mesial temporal sclerosis. J Neurol Neurosurg Psychiatry 80:312–319.

D'Arceuil HE, Westmoreland S, de Crespigny AJ (2007) An approach to high resolution diffusion tensor imaging in fixed primate brain. Neuroimage 35:553–565.

Focke NK, Yogarajah M, Bonelli SB, Bartlett PA, Symms MR, Duncan JS (2008) Voxel-based diffusion tensor imaging in patients with mesial temporal lobe epilepsy and hippocampal sclerosis. Neuroimage 40:728–737.

Gross DW, Concha L, Beaulieu C (2006) Extratemporal white matter abnormalities in mesial temporal lobe epilepsy demonstrated with diffusion tensor imaging. Epilepsia 47:1360–1363.

Gulani V, Webb AG, Duncan ID, Lauterbur PC (2001) Apparent diffusion

tensor measurements in myelin-deficient rat spinal cords. Magn Reson Med 45:191–195.

Harsan LA, Poulet P, Guignard B, Steibel J, Parizel N, de Sousa PL, Boehm N, Grucker D, Ghandour MS (2006) Brain dysmyelination and recovery assessment by noninvasive in vivo diffusion tensor magnetic resonance imaging. J Neurosci Res 83:392–402.

Johansen-Berg H, Behrens TE (2006) Just pretty pictures? What diffusion tractography can add in clinical neuroscience. Curr Opin Neurol 19:379–385.

Latour LL, Svoboda K, Mitra PP, Sotak CH (1994) Time-dependent diffusion of water in a biological model system. Proc Natl Acad Sci U S A 91:1229–1233.

Livy DJ, Schalomon PM, Roy M, Zacharias MC, Pimenta J, Lent R, Wahlsten D (1997) Increased axon number in the anterior commissure of mice lacking a corpus callosum. Exp Neurol 146:491–501.

Mac Donald CL, Dikranian K, Bayly P, Holtzman D, Brody D (2007) Diffusion tensor imaging reliably detects experimental traumatic axonal injury and indicates approximate time of injury. J Neurosci 27:11869–11876.

McDonald CR, Ahmadi ME, Hagler DJ, Tecoma ES, Iragui VJ, Gharapetian L, Dale AM, Halgren E (2008) Diffusion tensor imaging correlates of memory and language impairments in temporal lobe epilepsy. Neurology 71:1869–1876.

Mori S, Crain BJ, Chacko VP, van Zijl PC (1999) Three-dimensional tracking of axonal projections in the brain by magnetic resonance imaging. Ann Neurol 45:265–269.

Nilsson D, Go C, Rutka JT, Rydenhag B, Mabbott DJ, Snead OC 3rd, Raybaud CR, Widjaja E (2008) Bilateral diffusion tensor abnormalities of temporal lobe and cingulate gyrus white matter in children with temporal lobe epilepsy. Epilepsy Res 81:128–135.

Ozdogmus O, Cavdar S, Ersoy Y, Ercan F, Uzun I (2009) A preliminary study, using electron and light-microscopic methods, of axon numbers in the fornix in autopsies of patients with temporal lobe epilepsy. Anat Sci Int 84:2–6.

Rodrigo S, Oppenheim C, Chassoux F, Golestani N, Cointepas Y, Poupon C, Semah F, Mangin JF, Le Bihan D, Meder JF (2007) Uncinate fasciculus fiber tracking in mesial temporal lobe epilepsy. Initial findings. Eur Radiol 17:1663–1668.

Saksena S, Husain N, Das V, Pradhan M, Trivedi R, Srivastava S, Malik GK, Rathore RK, Sarma M, Pandey CM, Gupta RK (2008) Diffusion tensor imaging in the developing human cerebellum with histologic correlation. Int J Dev Neurosci 26:705–711.

Sankoh AJ, Huque MF, Dubey SD (1997) Some comments on frequently used multiple endpoint adjustment methods in clinical trials. Stat Med 16:2529–2542.

Schmierer K, Wheeler-Kingshott CAM, Boulby PA, Scaravilli F, Altmann DR, Barker GJ, Tofts PS, Miller DH (2007) Diffusion tensor imaging of post mortem multiple sclerosis brain. Neuroimage 35:467–477.

Schmierer K, Wheeler-Kingshott CAM, Tozer DJ, Boulby PA, Parkes HG, Yousry TA, Scaravilli F, Barker GJ, Tofts PS, Miller DH (2008) Quantitative magnetic resonance of postmortem multiple sclerosis brain before and after fixation. Magn Reson Med 59:268–277.

Schoene-Bake JC, Faber JC, Trautner P, Kaaden S, Tittgemeyer M, Elger CE, Weber B (2009) Widespread affections of large fiber tracts in postoperative temporal lobe epilepsy. Neuroimage 46:569–576.

Schwartz ED, Cooper ET, Fan Y, Jawad AF, Chin CL, Nissanov J, Hackney DB (2005) MRI diffusion coefficients in spinal cord correlate with axon morphometry. Neuroreport 16:73–76.

Simonyan K, Tovar-Moll F, Ostuni J, Hallett M, Kalasinsky VF, Lewin-Smith MR, Rushing EJ, Vortmeyer AO, Ludlow CL (2008) Focal white matter changes in spasmodic dysphonia: a combined diffusion tensor imaging and neuropathological study. Brain 131:447–459.

Song SK, Sun SW, Ramsbottom MJ, Chang C, Russell J, Cross AH (2002) Dysmyelination revealed through MRI as increased radial (but unchanged axial) diffusion of water. Neuroimage 17:1429–1436.

Song SK, Sun SW, Ju WK, Lin SJ, Cross AH, Neufeld AH (2003) Diffusion tensor imaging detects and differentiates axon and myelin degeneration in mouse optic nerve after retinal ischemia. Neuroimage 20:1714–1722.

Takahashi M, Hackney DB, Zhang G, Wehrli SL, Wright AC, O'Brien WT, Uematsu H, Wehrli FW, Selzer ME (2002) Magnetic resonance microimaging of intraaxonal water diffusion in live excised lamprey spinal cord. Proc Natl Acad Sci U S A 99:16192–16196.

Tukey JW, Ciminera JL, Heyse JF (1985) Testing the statistical certainty of a response to increasing doses of a drug. Biometrics 41:295–301.

Tyszka JM, Readhead C, Bearer EL, Pautler RG, Jacobs RE (2006) Statistical diffusion tensor histology reveals regional dysmyelination effects in the shiverer mouse mutant. Neuroimage 29:1058–1065.

Wu Q, Butzkueven H, Gresle M, Kirchhoff F, Friedhuber A, Yang Q, Wang H, Fang K, Lei H, Egan GF, Kilpatrick TJ (2007) MR diffusion changes correlate with ultra-structurally defined axonal degeneration in murine optic nerve. Neuroimage 37:1138–1147.

Yogarajah M, Powell HWR, Parker GJM, Alexander DC, Thompson PJ, Symms MR, Boulby P, Wheeler-Kingshott CA, Barker GJ, Koepp MJ, Duncan JS (2008) Tractography of the parahippocampal gyrus and material specific memory impairment in unilateral temporal lobe epilepsy. Neuroimage 40:1755–1764.